ULTIMATE LIMIT CAPACITY OF THIN-WALLED COLD-FORMED STEEL MEMBERS

VIOREL UNGUREANU[1], MARIA KOTEŁKO[2], DAN DUBINA[1]

Abstract. This paper is a review of research done in the recent years as a result of collaboration between the Department of Steel Structures and Structural Mechanics of the Politehnica University of Timisoara, Laboratory of Steel Structures of the Romanian Academy and Department of Strength of Materials of the Łódź University of Technology related to load carrying capacity, post-failure behaviour and plastic mechanisms of failure of thin-walled cold-forms steel (TWCFS) members subjected to compression and/or bending.

Key words: Thin-walled cold-formed steel members, Plastic mechanisms, Compression and/or bending, Experimental tests, Numerical simulations.

1. INTRODUCTION

The EN 1993-1-1 [1] code defines four classes of cross-sections of steel structural elements as shown in Figure 1. The role of cross-section classification is to identify the extent to which the resistance and rotation capacity of cross-sections is limited by its local buckling resistance.

Class 1 cross-sections are those which can form a plastic hinge with the rotation capacity required from plastic analysis without reduction of the resistance. Class 2 cross-sections are those which can develop their plastic moment resistance, but have limited rotation capacity because of local buckling, while Class 3 cross-sections are those in which the stress in the extreme compression fiber of the steel member assuming an elastic distribution of stresses can reach the yield strength, but local buckling is liable to prevent development of the plastic moment resistance. Class 4 cross-sections are those in which local buckling will occur before the attainment of yield stress in one or more parts of the cross-section. Consequently, for Class 4 cross-sections effective widths may be used to make the necessary allowances for reductions in resistance because of local buckling [1]. Thin-walled cold-formed steel (TWCFS) structures are usually made of thin-walled members of Class 4 sections.

[1] Politehnica University of Timisoara, Department of Steel Structures and Structural Mechanics / Romanian Academy - Timisoara Branch, Laboratory of Steel Structures, Romania

[2] Łódź University of Technology, Department of Strength of Materials, Poland

Ro. J. Techn. Sci. – Appl. Mechanics, Vol. 63, N° 3, P. 183–206, Bucharest, 2018

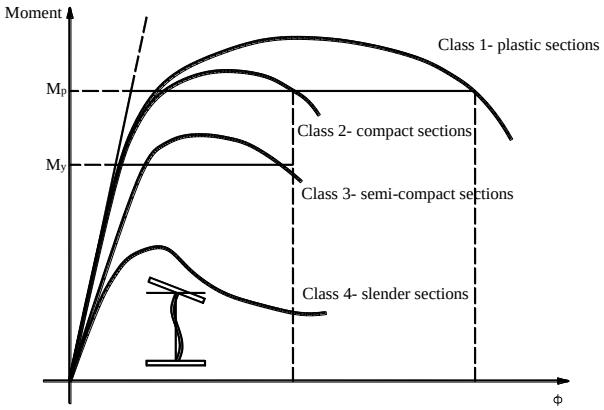

Fig. 1 – Cross-section behavior classes.

Since these sections are prematurely prone to local or distortional buckling and they do not have a real post-elastic capacity, a failure of members is initialized by the local-global interactive buckling of plastic-elastic type, not an elastic-elastic one. Thus, the failure at ultimate stage of those members, either in compression or bending, always occurs by forming a local plastic mechanism (see Figure 2).

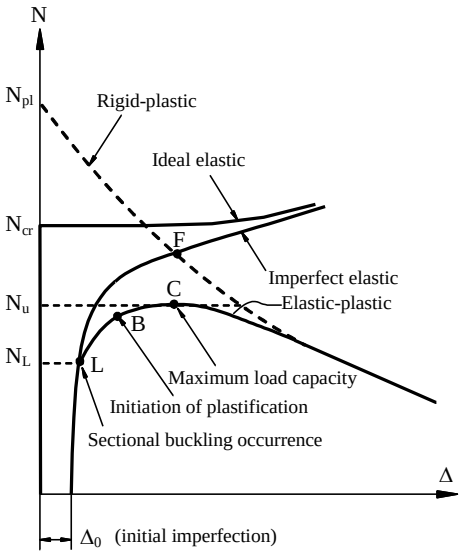

Fig. 2 – Structural behavior of TWCFS member subjected to compression.

This fact suggests the possibility to use the local plastic mechanism analysis to characterize the ultimate strength of such members, since an approximate upper-bound estimation of the load-carrying capacity of those members is the intersection point of the rigid-plastic curve and imperfect elastic one (point F in Figure 2).

There are two major classes of plastic mechanisms i.e. true mechanism and quasi-mechanism. A true mechanism is one which is developed from the original thin-walled member by folding the individual plates along the plastic hinge lines. A quasi-mechanism is one which in some regions of the individual plates of the structure is deformed by yielding in order to allow the plasticized zones to deflect. The mechanism type depends on the yield strength of steel, b/t slenderness ratio and the magnitude of initial geometrical imperfections of component walls of the thin-walled steel member.

The main problem is to identify correctly the type of plastic mechanism to be used in analysis. In fact, when local buckling firstly appears, it always changes into a local plastic mechanism when the member fails (see Figure 3). Therefore, the local plastic mechanism model naturally describes the stub column or short beam behavior, which is not the case of effective width model. The intersection of the elastic curve and the rigid-plastic one can be used to estimate the ultimate strength of a thin-walled element considering the initial imperfections.

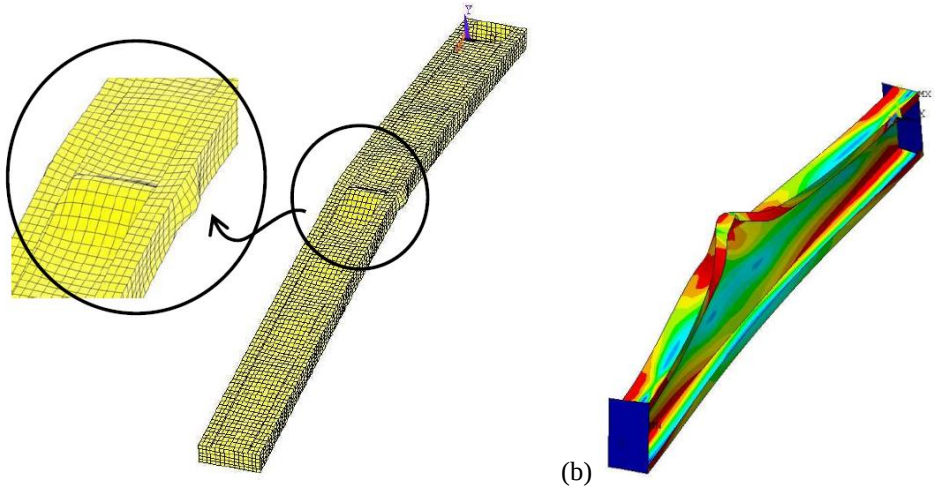

(a) (b)

Fig. 3 – FEM simulation of plastic-elastic interaction between the local plastic mechanism and global buckling for a lipped channel section in: (a) compression; (b) bending.

The load-carrying capacity of such members subjected to simple states of loading (pure bending or pure axial compression) is relatively well determined both based on the theory of thin-walled structures and in the code specifications. However, determination of the load-carrying capacity of TWCFS members subjected to combined load, particularly eccentric compression, is still an open question and the code specifications for that case should be improved. This improvement may be supported by developing adequate theoretical models of local plastic mechanisms.

This paper is a review of research done in the recent years as a result of

collaboration between the Department of Steel Structures and Structural Mechanics of the Politehnica University of Timisoara, Laboratory of Steel Structures of the Romanian Academy and Department of Strength of Materials of the Łódź University of Technology related to load carrying capacity, post-failure behavior and plastic mechanisms of failure of thin-walled cold-forms steel (TWCFS) members subjected to compression and/or bending.

2. STATE OF ART REVIEW

Experiments carried out by many researchers on beams or columns built from plate strips, subjected to uniform compression show that in such members some simple plastic mechanisms can be distinguished, which have been termed as basic mechanisms. Simultaneously, results of experiments performed, among others, by Murray & Khoo [2] confirmed that even a very complex mechanism can be described as the superposition of some simple basic mechanisms. Murray & Khoo [2] developed and classified 8 basic plastic mechanisms in plate strips under uniform compression. They also derived for each type of mechanism equations to describe the failure equilibrium path (load versus deflection). A database for plastic mechanisms for thin-walled cold-formed steel members in compression and bending has been presented in detail by Ungureanu et al. [3].

In the case of plates subjected to uniform compression, with symmetrical boundary conditions, which corresponds to the case of column web in compression, the basic plastic mechanisms, which may develop, are shown in Figure 4. The flip disc mechanism (see Figure 4a), was originally developed by Mahendran [4] and is described in detail by Kotełko [5]. The pitched-roof mechanism has been described by some researchers, i.e. Kato [7], Korol & Sherbourne [7], as well as Sin [8] and Mahendran [4]. The pyramid mechanism (see Figure 4c) was described by Ungureanu et al. [5].

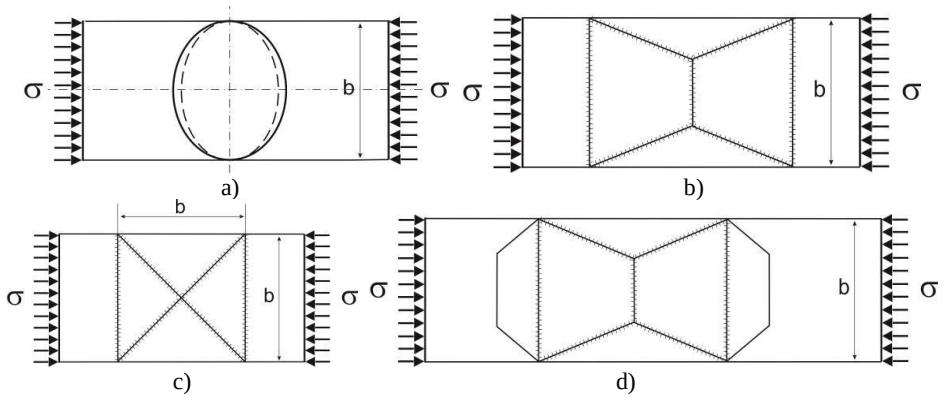

Fig. 4 – Basic plastic mechanisms in thin plates subjected to uniform compression:
a) flip disc, b) pitched-roof, c) pyramid, d) roof.

Modifications of pitched-roof mechanism and roof mechanism were developed by Rondal & Maquoi [9] and Kragerup [10]. The plastic mechanism approach of the above-mentioned mechanisms, using the energy method or the equilibrium strip method, were described in detail together with corresponding failure equilibrium path equations (load vs. deflection) by Kotełko [5].

Five plastic mechanisms of failure in channel section columns subjected to axial compression were originally developed by Murray & Khoo [2], as shown in Figure 5. Mechanisms CW1 and CW2 correspond to the case of the web in compression, while mechanisms CF1, CF2 and CF3 to the case of the flanges in compression. The CW1 and CW2 are web mechanisms, in fact, similar to flip disc (CW1) and roof (CW2) mechanisms. They were also analyzed by Dubina & Ungureanu [11], who described the mechanism CW2, and by Rasmussen & Hancock [12], who analyzed the mechanisms CF2 and CF3. In the papers mentioned above the equilibrium strip method has been applied.

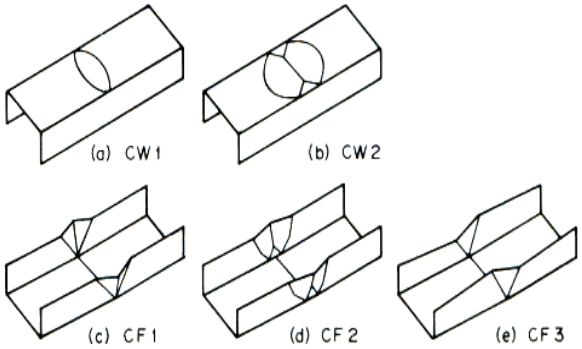

Fig. 5 – Basic plastic mechanisms of plain channels [2].

3. FUNDAMENTALS OF YIELD-LINE ANALYSIS

The rigid-plastic theory related to steel structures, based on the rigid-plastic material characteristics, was initially applied to the analysis of simple beams and frames [13]. In the 70's the research has been extended to investigate and characterize the plastic mechanisms of steel members. The term "yield line" was initially used by Jones & Wood [14]. The yield line theory applied to thin-walled steel structures allows one to perform an analysis of structural behavior in the vicinity of ultimate load and in the post-failure stage. The basic assumption is that the plastic mechanism is fully developed, and the plastic zones developed in the walls of thin-walled steel member are concentrated at yield lines, either stationary or travelling. At the level of yield lines, the material is considered fully plastic. Initially, the strain hardening was neglected in the analysis. Later, the modified yield line theory [15] considers this phenomenon.

If a plastic mechanism is fully developed, we can assume that the flat parts of the walls (created by yield lines) are non-deformed (there are no membrane deformations) and continuous. In that case, it is so-called "true mechanism" [16]. However, in many cases (determined by the geometry of the member and loading conditions), the true mechanisms do not describe properly the plastic mechanisms. The so-called "quasi-mechanism" are developed [16], where the flat parts of the walls are limited by yield lines but, the walls undergo membrane deformation.

The plastic mechanism approach is based on two basic methods, the *energy method (work method)* and the *equilibrium strip method* [5,17]. Using the energy method, the Principle of Virtual Velocities is applied, having the following form:

$$P \cdot \dot{\delta} = \int_V \sigma_{ij} \dot{\varepsilon}_{ij}^{p}(\beta, \chi) \mathrm{d}V \tag{1}$$

where P is generalized load, δ is the global generalized displacement, $\dot{\delta}$ is the rate of change of the global generalized displacement, β is the vector of kinematical parameters of the plastic mechanisms (kinematical admissible displacements), χ is vector of geometrical parameters of the plastic mechanisms, σ_{ij} is the stress tensor and $\dot{\varepsilon}_{ij}^{p}$ is the strain rate tensor.

Usually, in the analysis concerning thin-walled members subjected to compression, Eq. (1) is rearranged into the following form:

$$\delta W_{ext} = \delta W_b + \delta W_m \tag{2}$$

where δW_{ext} is the variation of work of external forces, δW_b is the variation of the energy of bending plastic deformation, while δW_m is the variation of the energy of membrane plastic deformation. Eq.(2) provides a relation of generalized load (e.g. compressive load, bending moment) in terms of general displacement (e.g. shortening, the angle of rotation). The graphical representation of this relation will be termed in the present paper as a post-failure curve. Alternatively, Eq.(2) may be rearranged into the following form:

$$P = \frac{\partial (W_b + W_m)}{\partial \delta} \tag{3}$$

The equilibrium strip method treats the plastic mechanism as a compatible collection of strips of infinite small or unit width parallel to the direction of applied force. Based on the free-body diagram of a separated strip an equilibrium equation is formulated and then, those equations are integrated across the walls of the plastic mechanism, in order to obtain simultaneous equilibrium equation for the mechanism as a whole [2]. An application of this method is restricted to the analysis of local plastic mechanisms build of stationary yield lines only. It is widely used in investigations of plated columns under compression and delivers a direct relation between the applied force and the deflection of the column.

A comparative study has been carried out by Flockhart et al. [17], who analyzed a thin-walled spot-welded box-section beam. He has concluded that for large rotations of the mechanism (global plastic hinge), the energy absorption determined by the energy method is higher up to 30% than that determined by the equilibrium strip method. The further investigation related to the comparison of those two approaches has been made by Kotełko et al. [18] and Kotełko & Mania [19]. A discussion of different solutions based on both methods was carried out by Zhao [20].

4. PLASTIC MECHANISMS OF TWCFS MEMBERS UNDER COMPRESSION

As mentioned, theoretical models of 3D plastic mechanisms of plain channel section columns were originally elaborated by Murray & Khoo [2]. Among them a true mechanism (three-hinge flange mechanism), which develops due to axial compression and/or bending (flanges deflect laterally towards the free edge – CF1 in Figure 5) has been developed.

If a plain channel is subject to bending or eccentric compression, the web being in compression, a web mechanism can develop. Murray and Khoo distinguished two quasi-mechanisms of that kind, namely flip disc (CW1 in Figure 5) and roof (CW2 in Figure 5). The web mechanism is in fact that one, which develops in the plate subjected to uniform compression, with symmetric boundary conditions. Basic plastic mechanisms in such plates are described in detail by Królak [21] and Ungureanu et al. [3]. Two of those mechanisms, namely the "pitched-roof" and "roof" one, have been presented in Figure 4.

Also, in the case of compression and/or bending, the flange being in compression, Murray & Khoo developed two other mechanisms, i.e. a true mechanisms CF3 (in Figure 5) and a quasi-mechanism CF2 (in Figure 5).

Some specific problems appear in the buckling and post-buckling analysis of TWCFS open section mono-symmetric members with edge stiffeners, because of rapid transition from symmetric to anti-symmetric buckling mode for certain buckling lengths, for which local-distortional buckling modes may take place. These buckling modes influence significantly the member's post-buckling and failure behaviour. Detailed elastic buckling and post-buckling analysis of such members was carried out by Kotełko et al. [22,23].

Let us consider two sections with edge stiffeners in and out, i.e. lipped channel (Figure 5a) and top hat (Figure 5b), subjected to uniform compression.

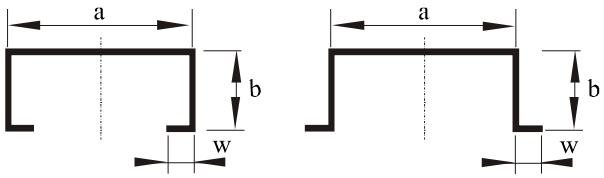

Fig. 6 – Members with edge stiffeners: a) lipped channel section, b) top hat section.

The plastic mechanism for columns with lipped channel sections subjected to uniform compression was proposed in [3,24,25]. The mechanism shown in Figure 7 consists of local roof mechanisms (CW2) in the web and flanges. In some solutions, local true mechanisms CF1 in lips were considered.

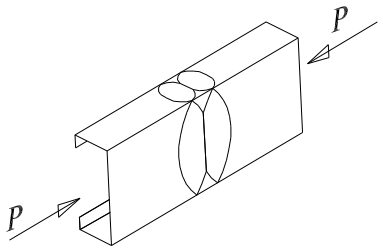

Fig. 7 – Plastic mechanism of failure for lipped channel section in compression.

Two plastic mechanisms for lipped channel sections under uniform compression were developed by Morino et al. [26], as shown in Figure 8.

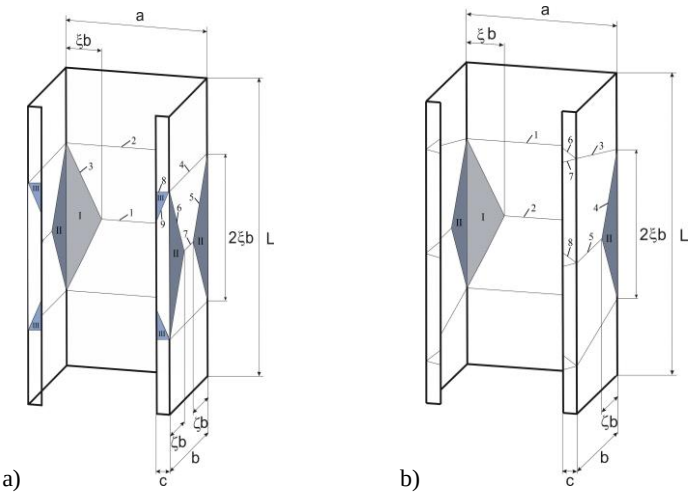

Fig. 8 – Theoretical models of: a) “triple-roof” mechanisms, b) CF-quasi-mechanism.

The "triple-roof" mechanism, presented in Figure 8a, is in fact a combination of pitched-roof mechanisms (Figure 4b) in the web and flanges and local CF1 (see Figure 5) mechanisms in lips. The CF-quasi-mechanism (see Figure 8b) consists of the local "pitched-roof" mechanism in the web and two local mechanisms similar to CF2 in the flanges, as well as local CF1 mechanisms in lips (see Figure 5). What kind of mechanism develops depends mainly on the buckling mode, which is induced by length-to-width ratio.

In the case of short top hat columns, for certain range of web-to-flange ratio, subjected to uniform compression or bending, numerical FE calculations and experimental tests results indicate different types of plastic mechanisms (see Figure 9a). Its theoretical model is shown in Figure 9b [22].

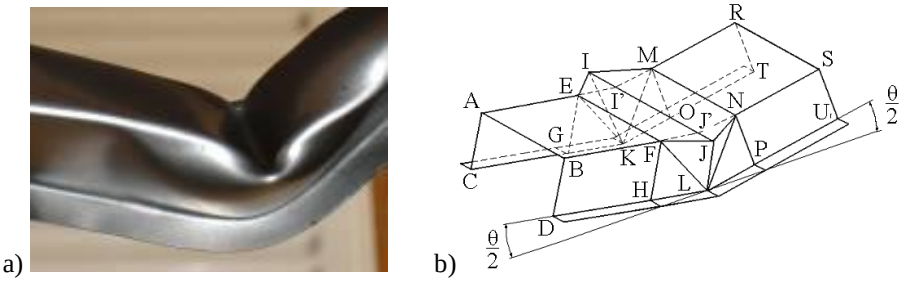

Fig. 9 – Plastic mechanism of failure for a top hat section [22]:
a) real mechanism of failure (quasi-static test), b) theoretical model.

Figure 10 provides numerical and experimental evidences of plastic mechanism of failure of cold-formed steel sections in compression. If compares these failure mechanisms with those of Figures 7 to 9, the similarity can be easily observed.

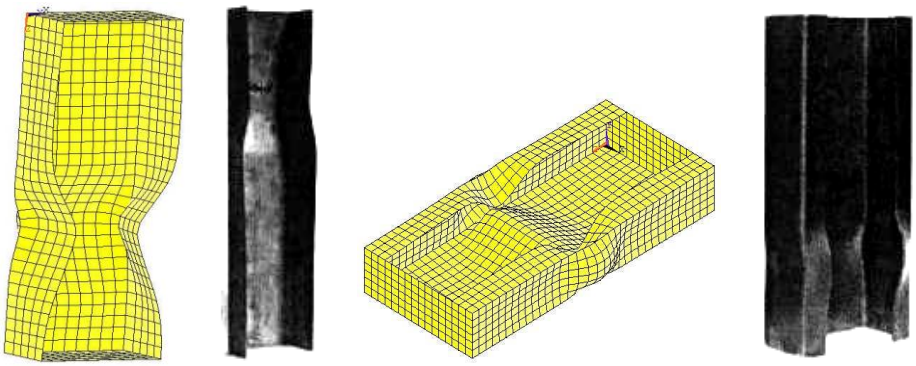

Fig. 10 – Numerical and experimental evidences of plastic mechanism failure
for members in compression.

5. PLASTIC MECHANISMS OF TWCFS MEMBERS UNDER BENDING

The authors of the paper evaluated the bending moment capacity of the global plastic hinge using the energy method, similar as Kecman [27] and Kotelko [28,29]. The energy absorbed during rotation of the global plastic hinge is the sum of three components:

$$W(\theta) = \sum_i W_1^{(i)} + W_2 + W_3 . \tag{4}$$

The first component of the above expression is a sum of energy absorbed during relative rotation of hinge walls along yield lines, which can be assumed to have a rolling radius equal to zero. Two other parts of the plastic energy consists of the energy of deformation of the plastic hinges, i.e. the corners of the global plastic mechanism.

The plastic moment of the global plastic hinge derived numerically is as follows:

$$M(\theta) = \frac{W(\theta + \Delta\theta) - W(\theta - \Delta\theta)}{2\Delta\theta} . \tag{5}$$

Figure 11 shows the local plastic mechanisms available for plain and lipped channel sections subjected to bending. They are based on the models proposed by Kotełko [15]. Details concerning the procedure used to obtain the local plastic mechanism strength are given by Ungureanu [30].

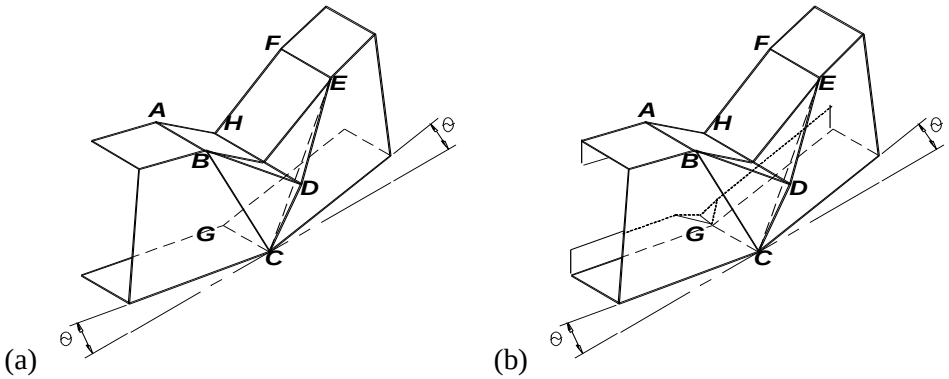

(a) (b)

Fig. 11 – Local plastic mechanisms for plain and lipped channel in bending [30].

Figure 12 provides experimental and numerical evidences of plastic mechanism of failure of cold-formed steel sections in bending, in a good agreement with the analytical models presented in Figure 11.

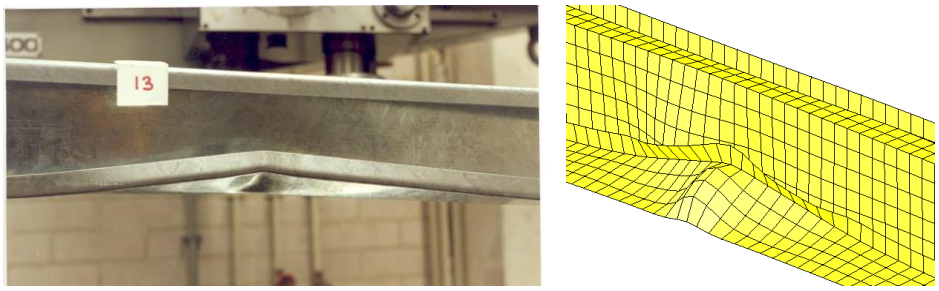

Fig. 12 – Numerical and experimental evidences of plastic mechanism failure for members in bending.

6. PLASTIC MECHANISMS OF TWCFS MEMBERS UNDER ECCENTRIC COMPRESSION

The first attempt at the identification of plastic mechanisms of short TWCFS members subjected to eccentric compression has been published by Ungureanu et al. [31]. In reference [31], two theoretical models have been developed only, based on plastic mechanisms obtained from numerical analyses, without considering the additional yield lines and tension fields in the flanges. Reference [32] confirmed and described in depth the plastic mechanisms of failure for the lipped channel section columns subjected to eccentric compression about the minor axis identified in [31]. Positive and negative eccentricities along the symmetry axis were investigated, as shown in Figure 13.

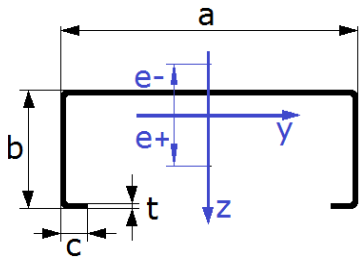

Fig. 13 – Lipped channel cross-section in eccentric compression.

The dimensions of the lipped channel cross-section investigated are $a \times b \times c \times t$ = 150×60×20×2 mm with and an internal radius r = 3 mm, as shown in Figure 13. The columns of length L = 450 mm were investigated, made of structural steel of yield stress f_y = 355 N/mm^2. Since the buckling mode influences on a large extent the failure mode of the compressed bar, the buckling behavior of examined columns was investigated. Buckling loads and modes were determined for the large range of eccentricities, from e = –60 mm to e = +100 mm. The analysis was carried out using CUFSM code [33] based on Finite Strip Method. For two cases (positive

and negative eccentricities) the FSM results were verified using an analytical-numerical method based on the asymptotic approach [34]. For positive eccentricities (e = 10, 30, 60, 100 mm) and e = –5 mm a typical distortional buckling takes place. For the negative eccentricity, e = –10 mm a local-distortional buckling mode was observed, while for eccentricities e = –30 mm and e = –60 mm the local buckling takes place.

Based on FE numerical experiments five plastic mechanisms of failure, as shown in Table 1, were identified.

Table 1

Failure mechanisms of 150×60×20×2 mm lipped channel [32]

Ecc. e [mm]	Buckling mode	Failure mode (mechanism)	Mechanism model	FE pattern
5 ÷ 20	Distortional	CF1	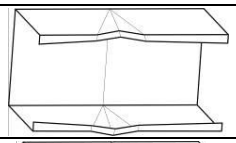	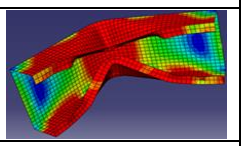
30 ÷ 40	Distortional	CF1/CF-quasi-mechanism	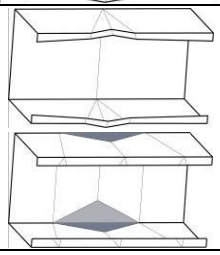	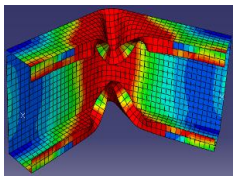
50 ÷ 100	Distortional	CF-quasi-mechanism	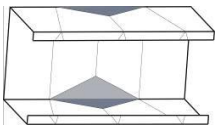	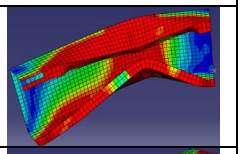
–5 ÷ -60	Local-distortional/ Local	Pitched-roof(I)	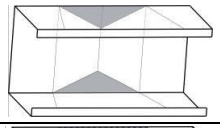	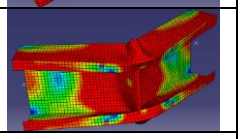
–100	Local	Roof/pitched roof	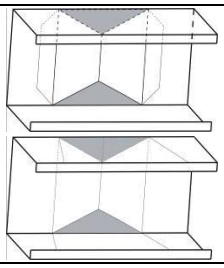	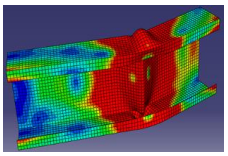

As shown in Table 1, for small positive eccentricities the true mechanism CF1, initiated by distortional buckling, originally developed by Murray & Khoo [2] was observed. For larger positive eccentricities (e = 30-100 mm) the CF quasi-mechanism, similar to that originally developed by Morino et al. [26] and to mechanism CF2 developed by Murray & Khoo [2] has been obtained.

For negative eccentricities (e = –5 … –60 mm), for which local-distortional or typical local buckling in the web takes place, a mechanism termed "pitched-roof(I)" was identified, which is a combination of the pitched-roof mechanism in the web and local mechanisms in the flanges (see Figure 8b). For the largest negative eccentricity (e = –100 mm) also the pitched-roof mechanism or roof mechanism was observed, as shown in Figure 4.

The detailed analytical descriptions of the five plastic mechanisms of failure presented above were presented in [32].

In order to investigate the applicability of the mechanisms presented above for members subjected to both positive and negative eccentricities, comparative numerical calculations have been carried out. The results of GMNIA analyses, performed with ABAQUS [35] code, were compared with post-failure curves obtained from the yield line analysis (YLA), using the energy method and/or the equilibrium strip method. For some selected cases the FE results and post-failure curves are compared with pre- and post-buckling paths derived from the analytical-numerical method (ANM) based on the asymptotic approach [34]. In those cases, an upper-bound estimation of the load-carrying capacity was performed as the intersection point of the post-buckling path and post-failure curve.

Figure 14 shows the comparison of load-shortening diagrams for the bar subjected to small positive eccentricities (e = 5, 10 mm) obtained from FE calculations, together with pre- and post-buckling paths derived from analytical-numerical (ANM) algorithm based on the asymptotic method [34] (for the eccentricity e = 10 mm only) and the failure curve, corresponding to CF1 mechanism, derived from energy method.

For small positive eccentricities, the mechanism CF1 gives a relatively good prediction of post-ultimate column behavior. Also, an upper-bound estimation of load-carrying capacity obtained from the intersection of post-buckling path and failure curve is in good agreement with FE prediction for the smallest eccentricity, i.e. e = 5 mm.

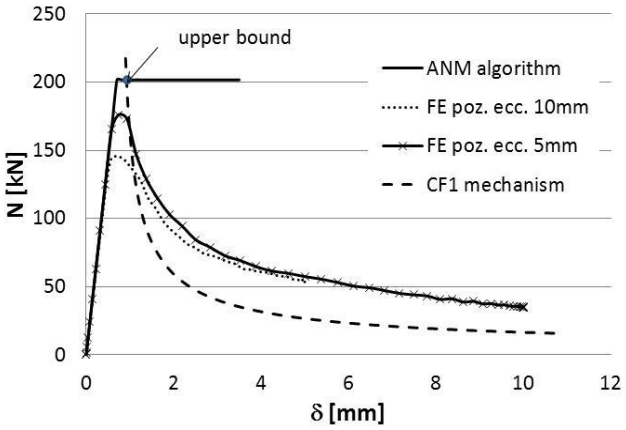

Fig. 14 – Load-shortening diagrams for small positive eccentricities; comparison of FE results and YLA analysis [32].

For larger positive eccentricities (see Table 1), the identified mechanism was the CF-quasi-mechanism. The post-failure paths for this mechanism were evaluated based on the theoretical model of this mechanism using the energy method. Geometrical parameters of this mechanism have been calibrated for each eccentricity and the agreement of YLA and FE results was very good.

For the smallest negative eccentricity (e = –5 mm) the YLA analysis was performed based on pitched-roof(I) mechanism theoretical model (see Figure 8a) with additional tension fields in the flanges. As shown, the YLA post-failure path overestimates the FE results. For medium negative eccentricities, compared with YLA analysis, together with pre- and post-buckling paths derived from analytical-numerical (ANM) algorithm (for eccentricity e = –60 mm only), the agreement of FE and YLA post-failure curves was good.

For large negative eccentricities, Figure 15 shows load-shortening diagrams obtained from FE simulation and YLA analysis (based on pitched-roof(I) mechanism). Also, in that case, the agreement is satisfactory. It should be underlined, that parameter ξ in the pitched-roof(I) mechanism model was calibrated according to a magnitude of the eccentricity.

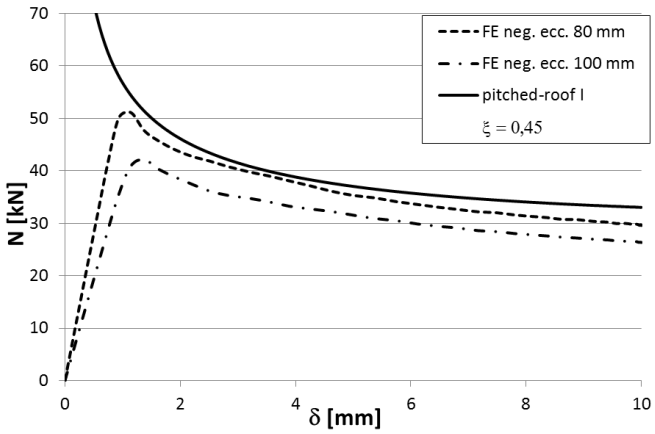

Fig. 15 – Load-shortening diagram for medium negative eccentricity; comparison of FE results and YLA analysis.

For the largest negative eccentricity (e = −100 mm) plastic mechanisms similar to pitched-roof and roof were observed. However, both post-failure curves obtained from YLA analysis based on those mechanisms are not in a good agreement with FE results. The theoretical models (pitched-roof and roof) are in fact web mechanisms models, which do not consider local mechanisms in the flanges and lips.

7. PLASTIC-ELASTIC INTERACTIVE BUCKLING VIA ECBL APPROACH

Cold-formed steel sections are traditionally considered with no plastic capacity, and consequently non-ductile, mainly due to wall slenderness involving local instability phenomena. However, even they do not have sufficient plastic rotation capacity to form plastic hinges, they can form local plastic mechanisms.

In case of thin-walled sections multiple local buckling modes may occur simultaneously under the same critical load. For a long member, multiple local buckling modes, e.g. m–1, m, m+1, characterized by L_{m-1}, L_m and L_{m+1} half wave lengths, may interact each other and give rise to an unstable post-critical behaviour called “localization of the buckling pattern” (see Figure 16).

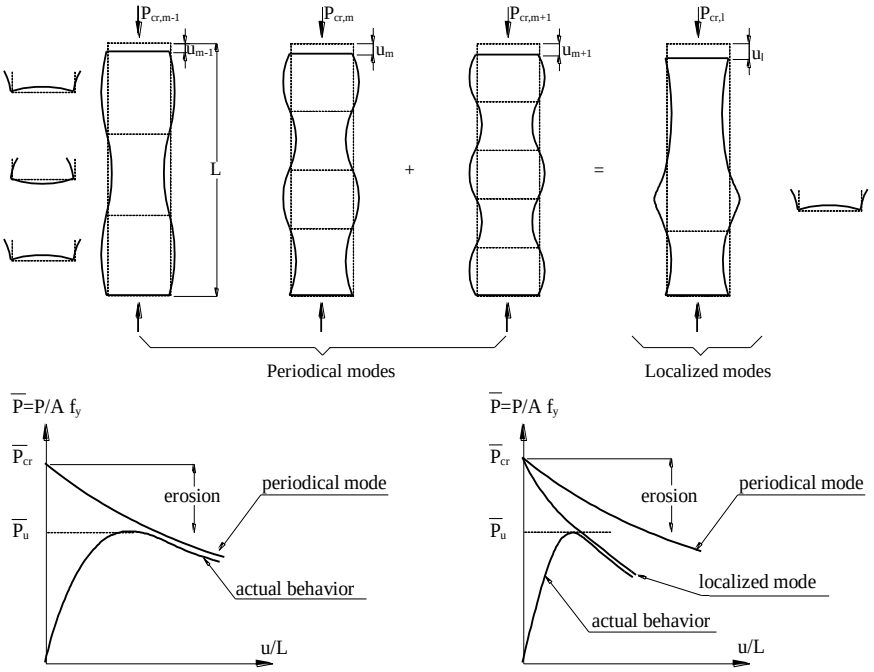

Fig. 16 – Periodical local modes and localization of buckling patterns in case of flanges of a plain channel section in compression.

The localized buckling mode is in fact an interactive or coupled mode. This is a "first" interaction, which may occur prior the overall buckling mode of the member. The "second" interaction, between the localized buckling mode and the overall one is dangerous because it is accompanied by a very strong erosion of critical bifurcation load. When localization of buckling patterns occurs, the member post-buckling behaviour is characterized by large local displacements, in the inelastic range, which produce the plastic folding of walls, and the member, falls into a plastic mechanism.

If the localized mode occurs prior to the overall one, the member post-buckling behaviour may be modified by material yielding and leads to a local plastic mechanism. In this case, the interaction occurs between the overall mode, which corresponds to an elastic non-linear behaviour of the thin-walled steel members, and the local plastic buckling of the component walls.

Based on the concept of Erosion of Critical Bifurcation Load (ECBL), Dubina [36] proposed an approach to evaluate the ultimate strength in local/distortional-global interactive buckling. This approach enables to use the Ayrton-Perry format of European buckling curves [37,38] to calibrate appropriate buckling curves for any kind of interactive local/distortional-global buckling. To illustrate the ECBL approach, let consider Figure 17 showing the typical theoretical

buckling curves of a thin-walled member in compression (black curves) and the actual one (green curve).

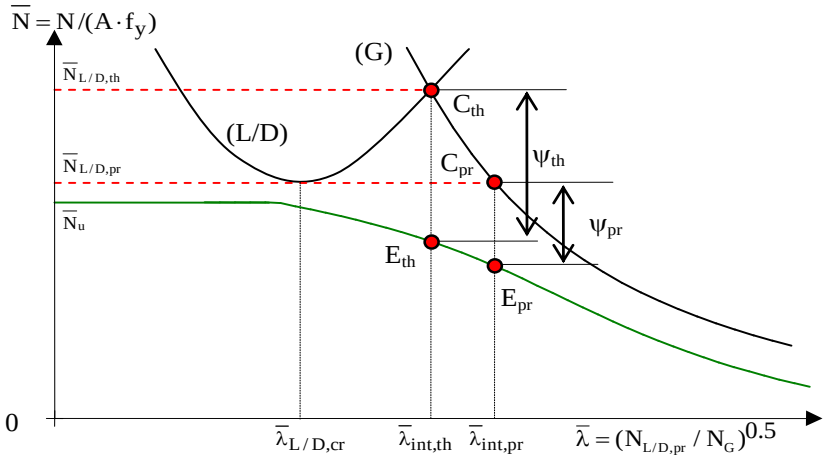

Fig. 17 – Interactive buckling model based on the ECBL approach.

In Figure 17, curve "G" denotes the quantities associated to global buckling modes, while curve "L/D" those associated to local/distortional ones. Moreover, $\overline{N}$ is the dimensionless axial force (being N the axial force and $A \cdot f_y$ the plastic strength of full cross-section) and $\overline{\lambda}$ is the dimensionless slenderness (being $\overline{N}_{L/D,pr}$ the smallest value between the non-dimensional local or distortional critical buckling load and the non-dimensional reduced section plastic resistance of the member, while N_G the critical global buckling load).

As it can be noted, global mode (G) interacts with local/distortional (L/D) one. The ECBL approach proposed by Dubina in [36] to evaluate the ultimate strength in global-local/distortional interactive buckling, hereinafter called ECBL$_{pr}$, is based on the main hypothesis that the reduction of the buckling load is most significant when the global buckling load is almost equal to the minimum value of local/distortional one [39,40]. In particular, in the ECBL$_{pr}$ the "practical interaction point", marked as C_{pr} in Figure 17, is assumed as the point where the erosion of the critical load, ψ_{pr}, is maximum. On the other hand, in the same graph it is also possible to identify the "theoretical interaction point", marked as C_{th}, corresponding to the intersection of the two buckling modes, and its related ψ_{th} erosion. The erosions can be expressed as follows:

$$\psi_* = 1 - \overline{N}_u / \overline{N}_{L/D,*} \tag{6}$$

where * can be *pr* or *th* and $\overline{N}_u$ is the dimensionless ultimate load.

In the framework of the ECBL$_{pr}$ approach, the Ayrton-Perry formula can be written as

$$\left(\overline{N}_{L/D,pr}-\overline{N}\right)\left(1-\overline{N}\bar{\lambda}^2\right)=\alpha_{pr}\overline{N}\left(\bar{\lambda}-0.2\right) \tag{7}$$

where α_{pr} is the imperfection factor. The solution of Eq. (7), in the coupling point, E_{pr} is:

$$\begin{aligned}\overline{N}=&\frac{1+\alpha_{pr}\left(\bar{\lambda}-0.2\right)+\overline{N}_{L/D,pr}\bar{\lambda}^2}{2\bar{\lambda}^2}-\\&-\frac{1}{2\bar{\lambda}^2}\sqrt{\left[1+\alpha_{pr}\left(\bar{\lambda}-0.2\right)+\overline{N}_{L/D,pr}\bar{\lambda}^2\right]^2-4\overline{N}_{L/D,pr}\bar{\lambda}^2}=\\&=\left(1-\psi_{pr}\right)\overline{N}_{L/D,pr}\end{aligned} \tag{8}$$

and considering

$$\bar{\lambda}=\frac{1}{\sqrt{\overline{N}_{L/D,pr}}} \tag{9}$$

it leads to

$$\alpha_{pr}=\frac{\psi_{pr}^2}{1-\psi_{pr}}\frac{\sqrt{\overline{N}_{L/D,pr}}}{1-0.2\sqrt{\overline{N}_{L/D,pr}}} \tag{10}$$

Starting from this real behaviour of thin-walled cold-formed steel stub columns and short beams, Ungureanu & Dubina [24,41] used the ECBL approach in order to express the plastic-elastic interactive buckling of thin-walled cold-formed steel members. The main problem of this approach is to evaluate properly the plastic strength of thin-walled members, via the local plastic mechanism theory and after, the erosion of critical load into the *"plastic-elastic coupling range"*.

Following the same way as for the elastic local-overall interactive buckling, it results the α imperfection factor for the plastic-elastic interactive buckling:

$$\alpha=\frac{\psi^2}{1-\psi}\cdot\frac{\sqrt{Q_{pl}}}{1-0.2\sqrt{Q_{pl}}} \tag{11}$$

where

$$Q_{pl} = \overline{N}_{pl,L} = \frac{N_{pl,m}}{A \cdot f_y} \tag{12}$$

and $N_{pl,m}$ is the local plastic mechanism strength.

In case of members in compression, Figure 18 presents the ECBL$_{pl\text{-}el}$ results [24,41], compared with those from FEM elastic-plastic analysis, the ECBL elastic-elastic, ECBL$_{el\text{-}el}$, and experimental tests [42]. EN 1993 – Part.1.3 and AISI-1996 results are also included in this comparison. Obviously, the quality of ECBL$_{pl\text{-}el}$ results is excellent, particularly in the interactive range, e.g. $0.4 < \overline{\lambda} < 1.6$.

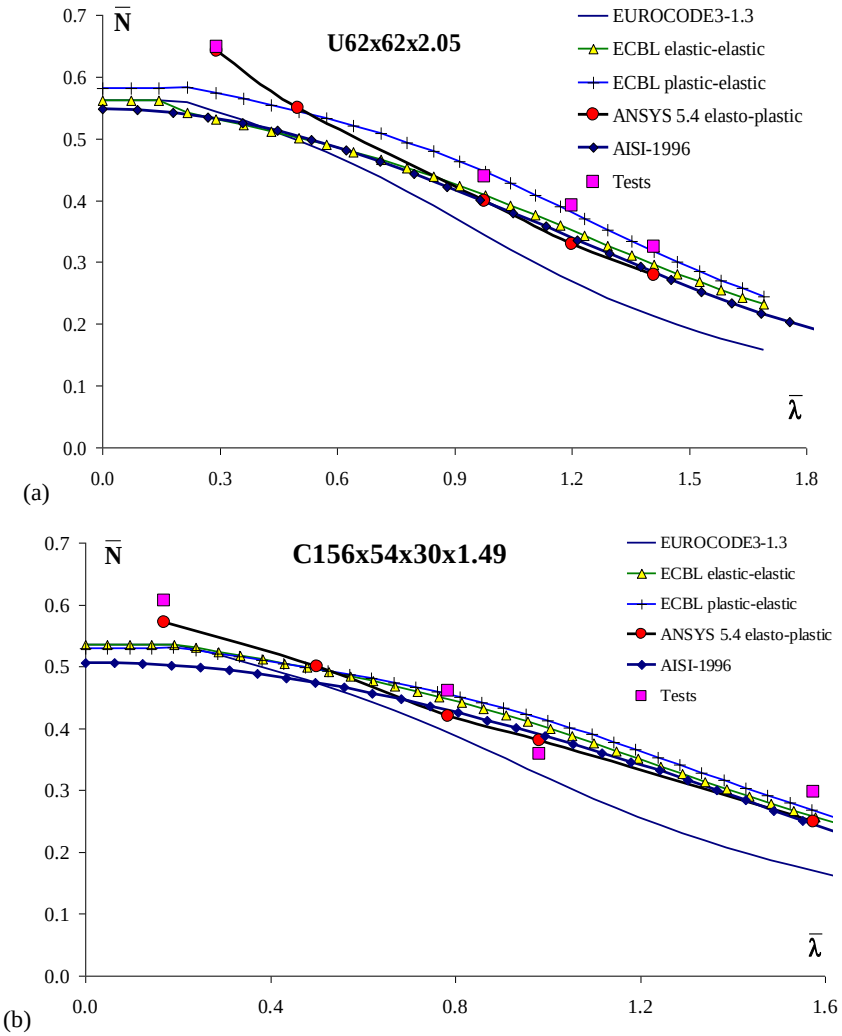

Fig. 18 – Numerical/Experimental comparison for compression members.

In case of slender beams, experimental data performed by Lovell [43] were used to compare the $ECBL_{pl\text{-}el}$ and $ECBL_{el\text{-}el}$ results with those of EN 1993 – Part.1.3 and AISI-1996 results. Figure 19 shows again that $ECBL_{pl\text{-}el}$ model confirms its accuracy [24, 41].

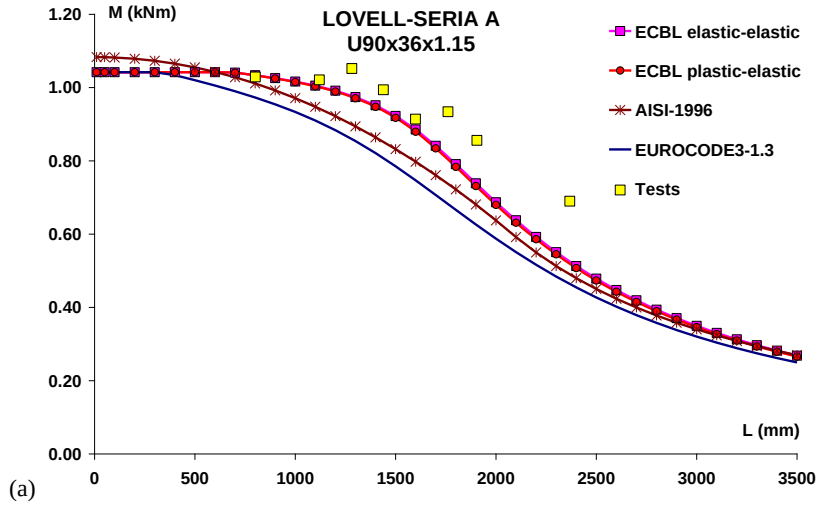

(a)

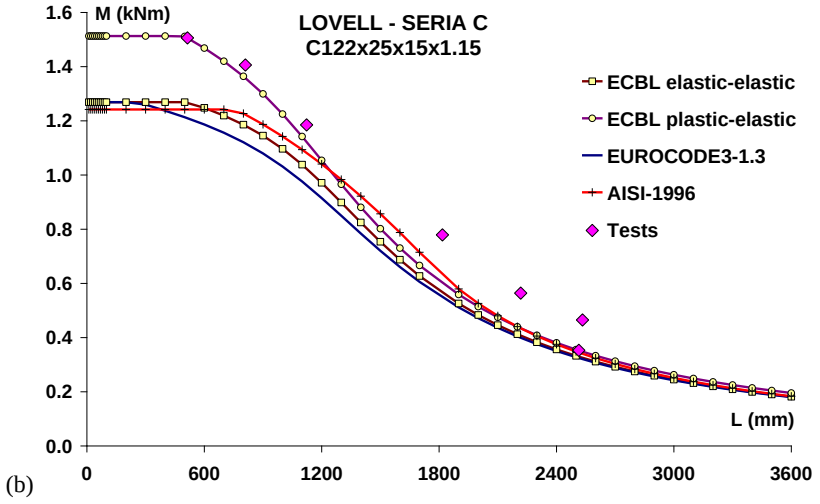

(b)

Fig. 19 – Numerical/Experimental comparison for bending members.

9. CONCLUSIONS

The local rigid-plastic model, describes properly the behaviour of thin-walled cold-formed steel short members. This model is consistent with the real phenomenon of stub columns and short beams failure and is confirmed by test results and advanced elastic-plastic FEM analysis.

The plastic-elastic interactive model naturally describes the phenomenon of the interactive buckling of thin-walled members. The ECBL plastic-elastic interactive approach, based on the erosion theory of coupled bifurcation, is much more rigorous and understandable than the semi-empirical methods used for the buckling curves in existing design codes.

The obtained results confirm the possibility to use the local plastic mechanism analysis to characterize the ultimate strength of short columns under compression, bending or eccentric compression.

Even if plastic mechanisms are identified for compression and bending separately, in the case of eccentric compression, this is far from a linear superposition of basic mechanisms. Generally, for certain eccentricity, an appropriate model of plastic mechanism should be calibrated based on FE simulation results and, simultaneously, by experimental results. Thus, further research into experimental verification of obtained theoretical results will be continued.

Even if the behaviour of longer members subjected to eccentric compression is not investigated in this paper, the *General method for lateral and lateral torsional buckling of structural components* presented in EN 1993-1-1 [1], adapted for this specific case, could be an alternative to estimate, in a more natural way, the capacity of such members based on plastic mechanisms.

The overall resistance to out-of-plane buckling for any structural component can be calculated/verified by ensuring that [1]:

$$\frac{\chi_{op}\alpha_{ult,k}}{\gamma_{M1}} \geq 1.0 \tag{13}$$

where:

$\alpha_{ult.k}$ is the minimum load amplifier of the design loads to reach the characteristic resistance of the most critical cross-section of the structural component considering its in-plane behavior without taking lateral or lateral-torsional buckling into account;

χ_{op} is the reduction factor for the non-dimensional slenderness $\bar{\lambda}_{op} = \sqrt{\alpha_{ult,k} / \alpha_{cr,op}}$, to take account of lateral and lateral-torsional buckling;

$\alpha_{cr.op}$ is the minimum amplifier for the in-plane design loads to reach the elastic critical load of the structural component with regards to lateral or lateral-torsional buckling without accounting for in-plane flexural buckling;

γ_{M1} is the safety coefficient ($\gamma_{M1} = 1$).

For the particular case presented above, the minimum load amplifier of the design loads, $\alpha_{ult.k}$, is obtained based on plastic mechanisms for members in eccentric compression about minor axis described in the previous paragraphs.

Acknowledgements. The research was supported by ROMANIAN–POLISH JOINT RESEARCH PROJECT "*Load-capacity of thin-walled steel members*" (2016-2018) under the agreement on scientific cooperation between the Romanian Academy and the Polish Academy of Sciences.

Received on November 3, 2018

REFERENCES

1. EN 1993-1-1:2005, *Eurocode 3: Design of steel structures - Part 1-1: General rules and rules for buildings*, European Committee for Standardization, Brussels, Belgium (including EN 1993-1-1:2005/AC, 2009).
2. MURRAY, N.W., KHOO, P.S., *Some basic plastic mechanisms in thin-walled steel structures*, Int. J. Mech. Sci., **23**, *12*, pp. 703–713, 1981.
3. UNGUREANU, V., KOTEŁKO, M., MANIA, R.J., DUBINA, D, *Plastic mechanisms database for thin-walled cold-formed steel members in compression and bending*, Thin-Walled Structures, **48**, *10-11*, pp. 818–826, 2010.
4. MAHENDRAN, M., *Local plastic mechanisms in thin steel plates under in-plane compression*, Thin-Walled Structure, **27**, *3*, 245–261, 1997.
5. KOTEŁKO, M., *Load-carrying capacity and mechanisms of failure of thin-walled structures*, WNT Warszawa (in Polish), 2010.
6. KATO, B., *Buckling strength of plates in the plastic range*, International Association of Bridge and Structural Engineering, **25**, pp. 127–141, 1965.
7. KOROL, R.M., SHERBOURNE, A.N., *Strength prediction of plates in uniaxial compression*, Journal of Structural Division, **98**, pp. 1965–1986, 1972.
8. SIN, K.W., *The collapse behaviour of thin-walled sections*, PhD Thesis, Dept. of Mechanical Engineering, University of Strathclyde, Glasgow, 1985.
9. RONDAL, J., MAQUOI, R., *Stub-column strength of thin-walled square and rectangular hollow sections*, Thin-Walled Structures, **3**, *1*, pp. 15–34, 1985.
10. KRAGERUP, J., *Five notes on plate buckling*, Technical University of Denmark, Department of Structural Engineering, Series R, No. 143, 1982.
11. UNGUREANU, V., DUBINA, D., *Recent research advances on ECBL approach. Part I: Plastic–elastic interactive buckling of cold-formed steel sections*, Thin Walled Structures, **42**, pp. 177–194, 2004.
12. RASSMUSSEN, K.J.R., HANCOCK, G.J., *Nonlinear analyses of thin-walled channel-section columns*, Thin-Walled Structures, **13**, *1-2*, pp. 145–176, 1991.
13. HORNE, M.R., *Plastic Theory of Structures*, Thomas Nelson & Sons, 1971.

14. JONES, L.L., WOOD, R.H., *Yield line analysis of slabs*, American Elsevier, New York, 1967.
15. KOTEŁKO, M., *Load-capacity estimation and collapse analysis of thin-walled beams and columns – Recent advances*, Thin-Walled Structures, **42**, *2*, pp. 153–175, 2004.
16. MURRAY, N.W., *Introduction to the theory of thin-walled structures*, Clarendon Press, Oxford, 1986.
17. FLOCKHART, C.J., MURRAY, N.W., GRZEBIETA, R.H., *Comparison of upper-bound rigid-plastic yield line mechanism analysis by the energy and equilibrium strip method*, Proc. of the 2nd Australasia Congress of Applied Mechanics, Canberra, Australia, Paper R053, 1999.
18. KOTEŁKO, M., UNGUREANU, V., DUBINA, D., MACDONALD, M., *Plastic strength of thin-walled plated members – Alternative solutions review*, Thin-Walled Structures, **49**, *5*, pp. 636–644, 2011.
19. KOTEŁKO, M., MANIA, R.J., *Alternative solution of the problem of load-capacity of thin-walled plated structures*, Mechanics and Mechanical Eng., **12**, *4*, pp. 323–336, 2008.
20. ZHAO, X-L., *Yield line mechanism analysis of steel members and connections*, Prog. Struct. Engng. Mater., **5**, pp. 252–262, 2003.
21. KRÓLAK M. [ed.], *Post-buckling and load-capacity of thin-walled girders of flat walls* (in Polish), PWN, Warszawa-Łódź, 1990.
22. KOTEŁKO, M., KOŁAKOWSKI, Z., MANIA, R., *Ultimate loads and collapse behaviour of thin-walled hat section columns under compression*, Proc. of the International Colloquium on Stability and Ductility of Steel Structures (SDSS'06), IST Press, pp. 267–273, Lisbon, September 6-8, 2006.
23. KOTEŁKO, M., KOLAKOWSKI, Z., RHODES, J., *Comparative investigation into buckling loads and load-bearing capacity of thin-walled columns under compression*, Lightweight Structures in Civil Engineering, Warsaw, pp. 206–210, 2005.
24. UNGUREANU, V., DUBINA, D., *Post-elastic strength and ductility of cold-formed steel sections*, Proceedings of the Fourth International Conference on Thin-Walled Structures, pp. 283–290, Loughborough, UK, June 22-24, 2004.
25. DUBINA, D., UNGUREANU, V., *Plastic strength of thin-walled members*, Proc. of the Sixteenth Int. Specialty Conference on Cold-Formed Steel Structures, pp. 324–332, Orlando, Florida, 2002.
26. MORINO, S., KAWAGUCHI, J., MIZUNO, Y., HANYA, K., *Distortional buckling of light-gauge lipped channel short columns*, Steel Structures, **3**, pp. 203–217, 2003.
27. KECMAN, D., *Bending collapse of rectangular and square section tubes*, International Journal of Mechanical Sciences, **25**, *9-10*, pp. 623–636, 1983.
28. KOTELKO, M., KROLAK, M., *Collapse behaviour of triangular cross-section girders subject to pure bending*, Thin-Walled Structures, **15**, *2*, pp. 127–141, 1993.
29. KOTELKO, M., *Ultimate load and post-failure behaviour of box-section beams under pure bending*, Engineering Transactions, **44**, *2*, pp. 229–251, 1996.
30. UNGUREANU, V., *Lateral-torsional buckling of thin-walled cold-formed beams*, PhD Thesis, The "Politehnica" University of Timisoara, Romania, 2003.
31. UNGUREANU, V., KOTEŁKO, M., GRUDZIECKI, J., *Plastic mechanisms for thin-walled cold-formed steel members in eccentric compression*, Acta Mechanica et Automatica, **10**, *1*, pp. 33–37, 2016.
32. UNGUREANU, V., KOTEŁKO, M., KARMAZYN, A., DUBINA, D., *Plastic mechanisms of thin-walled cold-formed steel members in eccentric compression*, Thin-Walled Structures, **128**, pp. 184–192, 2018.
33. LI, Z., SCHAFER, B.W., *Buckling analysis of cold-formed steel members with general boundary conditions using CUFSM: conventional and constrained finite strip methods*, Proc. of the 20th Int. Spec. Conf. on Cold-Formed Steel Structures, St. Louis, MO., USA, November 2010.

34. KOLAKOWSKI, Z., *A semi-analytical method for the analysis of the interactive buckling of thin-walled elastic structures in the second order approximation*, Int. J. Solids Structures, **33**, *25*, pp. 3779–3790, 1996.
35. ABAQUS/Standard Version 6.7-1, *ABAQUS Documentation*, Dassault Systèmes, Providence, RI, USA, 2007.
36. DUBINA, D., *The ECBL approach for interactive buckling of thin-walled steel members*, Steel & Composite Structures, **1**, *1*, pp. 75–96, 2001.
37. GIONCU, V., *General Theory of Coupled Instabilities*, Thin-Walled Structures, **19**, *2-4*, pp. 81–127, 1994.
38. RONDAL, J., MAQUOI, R., *Formulation d'Ayrton-Perry pour le flambement des barres métalliques*, Construction Métallique, **4**, pp. 41–53, 1979.
39. VAN DER NEUT, A., *The interaction of local buckling and column failure of thin-walled compression members*, Proceedings of the 12th Int. Congress on Applied Mechanics (Heteny M.K., Vincenti W.G. eds.), pp. 389–399, Berlin: Springer-Verlag, 1969.
40. DUBINA, D., UNGUREANU, V., *Instability mode interaction: from van der Neut model to ECBL approach*, Thin-Walled Structures, **81**, pp. 39–49, 2014.
41. UNGUREANU, V., DUBINA, D., *Recent research advances on ECBL approach. Part I: Plastic-elastic interactive buckling of cold-formed steel sections*, Thin-Walled Structures, **42**, *2*, pp. 177–194, 2004.
42. BATISTA, E., *Essais de profils C et U en acier plies a froid*, Rep. No. 157, Universite de Liege, Laboratoire de Stabilite des Constructions, 1986.
43. LOVELL, H.M., *Lateral buckling of light gauge steel beams*, MSc Thesis, University of Salford, 1985.